

# Nonrigid Registration Using Regularization that Accommodates Local Tissue Rigidity

Dan Ruan, Jeffrey A. Fessler<sup>a</sup>, Michael Roberson, James Balter and Marc Kessler<sup>b</sup>

<sup>a</sup> Department of Electrical Engineering & Computer Science.

<sup>b</sup> Department of Radiation Oncology.  
The University of Michigan, Ann Arbor, MI

## ABSTRACT

Regularized nonrigid medical image registration algorithms usually estimate the deformation by minimizing a cost function, consisting of a similarity measure and a penalty term that discourages “unreasonable” deformations. Conventional regularization methods enforce homogeneous smoothness properties of the deformation field; less work has been done to incorporate tissue-type-specific elasticity information. Yet ignoring the elasticity differences between tissue types can result in non-physical results, such as bone warping. Bone structures should move rigidly (locally), unlike the more elastic deformation of soft tissues. Existing solutions for this problem either treat different regions of an image independently, which requires precise segmentation and incurs boundary issues; or use an empirical spatial varying “filter” to “correct” the deformation field, which requires the knowledge of a stiffness map and departs from the cost-function formulation.

We propose a new approach to incorporate tissue rigidity information into the nonrigid registration problem, by developing a space variant regularization function that encourages the local Jacobian of the deformation to be a nearly orthogonal matrix in rigid image regions, while allowing more elastic deformations elsewhere.

For the case of X-ray CT data, we use a simple monotonic increasing function of the CT numbers (in HU) as a “rigidity index” since bones typically have the highest CT numbers. Unlike segmentation-based methods, this approach is flexible enough to account for partial volume effects. Results using a B-spline deformation parameterization illustrate that the proposed approach improves registration accuracy in inhale-exhale CT scans with minimal computational penalty.

**Keywords:** X-ray computed tomography (CT), regularization, homomorphism, orthogonal matrix, Frobenius norm

## 1. INTRODUCTION

Medical imaging is an essential component of a large number of clinical applications. Very often, information obtained from multiple images are of complementary nature, and spatial alignment is required to properly integrate useful information from separate images [1]. This procedure is called *registration*, which aims at retrieving the transformation  $T$  that maps from the reference image  $f$ 's coordinate space to the homologous image  $g$ 's coordinate space, such that  $f \approx g \circ T$ .

Registration algorithms can be classified according to the space that  $T$  belongs: (global) *rigid/affine* registration algorithms have only a few degrees of freedom, while nonrigid registration algorithms have a very high dimensional space for feasible transformations. Usually, rigid registration methods provide satisfactory matching results for bone structures, but are in general not descriptive enough for elastic tissues regions that can have more free-form deformations.

Nonrigid registration problems are highly under-determined due to the extremely high dimensionality of transformation field, and this results in ill-conditioning as well as instability of solutions and local optima issues. Regularizations are introduced to alleviate these issues and also to incorporate prior physiological knowledge into the problem formulation. Therefore, regularized nonrigid medical registration algorithms are usually set up to use a cost function, consisting of a similarity measure and a penalty term that discourages undesirable transformations. Conventional registration methods use homogeneous regularization for smoothness or incompressibility properties of the deformation field [2–4].

However, ignoring the elasticity difference between tissue types can result in non-physiological results, such as bone warping. Existing work addressing this issue either treats different regions of an image independently [5,6], which requires

---

Dan Ruan: E-mail: druan@eecs.umich.edu, Telephone: 734-936-4309  
Jeffrey A. Fessler: E-mail: fessler@umich.edu, Telephone: 734-763-1434

precise segmentation in the first place and incurs boundary issues that could cause discontinuity and nondifferentiability; or use an empirical spatial varying “filter” to “correct” the deformation field, which requires the explicit knowledge of a stiffness map and may desire further justification for an efficient filter design scheme [7].

This paper describes a new approach to utilize tissue-type-dependent rigidity information into nonrigid registration framework.

Section 2 proposes a novel method for the overall cost function design and in particular the tissue-type-dependent regularization function. Section 3 describes clinical data used in the validation experiment. Section 4 reports validation experiment and test results. We conclude with summary and discussions for further investigation in section 5.

## 2. OPTIMIZATION PROBLEM FORMULATION AND REGULARIZATION DESIGN

The goal of nonrigid registration is to find the transformation  $\mathbf{T}^*$  such that the transformed homologous image best matches the reference image. In this report, we denote with  $f, g : \Omega \rightarrow \mathbb{R}$ , where  $\Omega \subset \mathbb{R}^d$ , the intensity map for the reference image and homologous image respectively, where  $d$  is the dimensionality of imagery. The open set  $\Omega$  denotes the physical region of interest for registration. Let  $\mathbf{T} : \Omega \rightarrow \Omega$  be the transformation. Let  $\underline{x} \in \Omega$  denote the coordinate (in vector form) of a specific location. Our goal is to find:

$$\begin{aligned} \mathbf{T}^* &= \arg \min_{\mathbf{T} \in \Gamma} \Phi(\mathbf{T}, f, g) \\ &= \arg \min_{\mathbf{T} \in \Gamma} \{C(f, g \circ \mathbf{T}) + R(\mathbf{T})\}, \end{aligned} \quad (1)$$

where  $\Gamma$  is the class of allowable transformations. Here,  $\Phi$  is the overall objective function that we want to minimize, consisting of two parts:  $C(f, g \circ \mathbf{T})$  denotes the data (dis)similarity measure, and  $R(\mathbf{T})$  denotes the regularization term that we apply to penalize undesirable transformations.

### 2.1. $L_2$ norm for data (in)fidelity measure

We are interested in nonrigid registration problems for calibrated X-ray CT images in particular, where sum of squared difference ( $L_2$  norm) is a sensible choice to measure data similarity, *i.e.*,

$$C(f, g \circ \mathbf{T}) = \sum_{\underline{x} \in \Omega} (f(\underline{x}) - g(\mathbf{T}(\underline{x})))^2.$$

In our experimental result, we choose to use it as our data fidelity measure, although the regularization design method applies generally to other data similarity metrics as well.

### 2.2. Regularization Design

The regularization  $R(\mathbf{T})$  is composed of two parts: a homogeneous spatial roughness penalty for deformation field, and a spatial varying (inhomogeneous) penalty that accounts for local tissue rigidity. For parametrization purpose, our regularization design takes the deformation instead of the transformation itself as input. We denote the deformation field  $\mathbf{D} : \mathbb{R}^d \rightarrow \mathbb{R}^d \triangleq \mathbf{T} - \mathbf{I}$ . The homogeneous smoothness penalty is defined with the commonly used squared Frobenius norm as  $\|\nabla \mathbf{D}\|_{Frob}^2$ . A reasonable local tissue rigidity based penalty is  $\sum_{\underline{x}} \gamma(\underline{x})r(\mathbf{T}_{\underline{x}})$ , and the overall regularization becomes:

$$R(\mathbf{T}) = \gamma_s \|\nabla \mathbf{D}\|_{Frob}^2 + \sum_{\underline{x} \in \Omega} \gamma(\underline{x})r(\mathbf{T}_{\underline{x}}).$$

We can equivalently represent the penalty as a function of the deformation field, since there is a one-to-one correspondence between transformation and deformation:

$$R(\mathbf{D}) = \gamma_s \|\nabla \mathbf{D}\|_{Frob}^2 + \sum_{\underline{x} \in \Omega} \gamma(\underline{x})r(\mathbf{D}_{\underline{x}} + \mathbf{I}), \quad (2)$$

where  $r(\mathbf{D}_{\underline{x}} + \mathbf{I})$  penalizes the deviation of the local transformation from being rigid, and  $\gamma(\underline{x})$  is a spatial varying weight that reflects local tissue rigidity properties. In particular,  $\gamma(\underline{x})$  can be looked on as the *local* “trade-off” between intensity match and tissue rigidity condition. It should be large where bone structure lies and small within more elastic regions. We also call it “*local stiffness factor*” to illustrate its physical meaning.

### 2.2.1. Local Rigidity Functional

The next step is to design an appropriate non-rigidity penalty function. The following claims help define reasonable choices.

To design the proper functional  $r : (\mathbb{R}^d \rightarrow \mathbb{R}^d) \rightarrow \mathbb{R}^{\geq 0}$ , we make the following claim:

CLAIM 2.1. *A necessary and sufficient condition for a map  $T$  to be rigid at  $\underline{x}$  is that its Jacobian matrix  $J_T(\underline{x}) = \nabla T(\underline{x})$  be orthogonal.*

The proof is straight forward as follows:

The general isometry in  $\mathbb{R}^d$  includes rotation, translation, reflection, and arbitrary compositions of the previous operations. It is easy to check that isometry defined on  $\mathbb{R}^d \rightarrow \mathbb{R}^d$  is a well-defined group with group operation being the standard map composition and identity element  $e$  being the identity map  $I_d$ .

LEMMA 2.2. *If we define a map  $J : G \rightarrow O(d)$ , via  $J(g) \triangleq$  Jacobian matrix of  $g$  for  $g \in G$ .*

*where  $G$  denotes the group of isometries on  $\mathbb{R}^d$ , and  $O(d)$  being the orthogonal group in  $d$ -dimension, then  $J$  is a group homomorphism between  $G$  and  $O(d)$ .*

It is easy to check according to the definitions:

- The group operation is preserved:  $J(g_1 \circ_G g_2) = J(g_1) \circ_O J(g_2)$ .

The Jacobian matrix of the composition of a sequence of isometric maps is identical to the matrix multiplication (the group operation on  $O(d)$ ) of the Jacobian matrix of each isometry.

- The identity is mapped to identity:  $J(e_G) = e_O$ .

$e_G = I_d$  and its Jacobian is itself,  $J(I_d) = I_d = e_O$ .

Moreover, we know that the image  $J(G) = O(d)$ , and the group kernel  $J^{-1}(e_O) = \{\text{the set of translations}\}$ .

Lemma 2.2 shows the claim. Since if  $T_{\underline{x}} \in G$ , then  $J(T_{\underline{x}}) \in J(G) = O(d)$ . On the other hand, if  $J_T(\underline{x}) \in O(d)$ , then  $T_{\underline{x}} \bmod \{\text{the normal group of translations}\} = J_T(\underline{x})$ . But  $J_T(\underline{x}) \in O(n) \subset G$ , and  $G$  is closed under composition with translations, so the orbit of  $J_T(\underline{x})$  under all possible translations (the group kernel) is a proper subset of  $G$ , thus,  $T_{\underline{x}} \in G$ .

With the above claim, we have found a mathematically rigorous way to describe the deviation of the local transformation  $T_{\underline{x}}$  from being rigid. It suffices now to design a penalty that measures how “non-orthogonal” the Jacobian matrix of the local transformation  $J_T(\underline{x})$  is.

We use the following fact:

LEMMA 2.3. *A necessary and sufficient condition for a matrix  $M \in \mathbb{R}^{d \times d}$  to be orthogonal is that  $\|MM^T - I_d\| = 0$ , where  $\|\cdot\|$  denotes any matrix norm.*

Notice that if  $M$  is orthogonal, then  $MM^T = I_d$ , and  $\|MM^T - I_d\| = 0$  for any norm. On the other hand, for any matrix norm,  $\|MM^T - I_d\| = 0$  implies  $MM^T = I_d$ , which is exactly the definition for the matrix  $M$  to be orthogonal.

For simplicity, we choose to use the squared Frobenius norm, and design the rigidity regularization function to be:

$$r(T_{\underline{x}}) \triangleq \|J(T_{\underline{x}})J(T_{\underline{x}})^T - I_d\|_{\text{Frob}}^2,$$

or equivalently,

$$\begin{aligned} r(D_{\underline{x}}) &= \|J(D_{\underline{x}} + I_d)J(D_{\underline{x}} + I_d)^T - I_d\|_{\text{Frob}}^2 \\ &= \| (J(D_{\underline{x}}) + I_d)(J(D_{\underline{x}}) + I_d)^T - I_d \|_{\text{Frob}}^2 \\ &= \| J(D_{\underline{x}})J(D_{\underline{x}})^T + J(D_{\underline{x}}) + J(D_{\underline{x}})^T \|_{\text{Frob}}^2. \end{aligned} \quad (3)$$

### 2.2.2. Local Stiffness Factor

To design the spatial varying local stiffness factor  $\gamma(\underline{x})$ , which determines the relative weighting between data infidelity and deviation from rigidity, it is desirable to have it as a monotone increasing (nondecreasing) function of the rigid level of the local tissue. Ideally, we would like to have it to reflect the relative elasticity among different tissue types, but since we are not aware of any exact quantitative description of this type, the described monotonicity relationship is the best we can hope for.

FACT 1. *In calibrated X-ray CT images, pixel intensity (CT number) is highly correlated with tissue type information, hence a good inference source for local rigidity.*

Therefore, instead of designing a direct map  $\gamma : \Omega \rightarrow \mathbb{R}^+$ , we define the local stiffness factor as an implicit function that is the composition of a monotone increasing function and the image intensity map:

$$\gamma(\underline{x}) = h(f(\underline{x})),$$

where  $h : \mathbb{R} \rightarrow \mathbb{R}^+$  is a monotone increasing map from the domain of CT number to rigidity level. We choose to use a scaled and shifted hyperbolic tangent function in our application due to its simplicity (two parameters with clear shape meaning), sharp rising edge and desirable situation behavior in bone structures.

In Fig. 1, we plot the empirical histogram taken from a  $192 \times 160 \times 60$  breath-held thorax CT volume with voxel size  $0.2 \times 0.2 \times cm^3$ . Observations for the tissue type v.s. CT number (in Hounsfield unit) relationship agree with theoretical values [8] in that:

Air	:	-1000Hu
Fat	}	: -100 ~ 60Hu
Muscle	}	
Bones	:	250 ~ 1000Hu.

We choose the location and shape parameters for the hyperbolic function such that the rigidity penalty becomes strong and more dominant when in the bony structure, while much relaxed within elastic tissues.

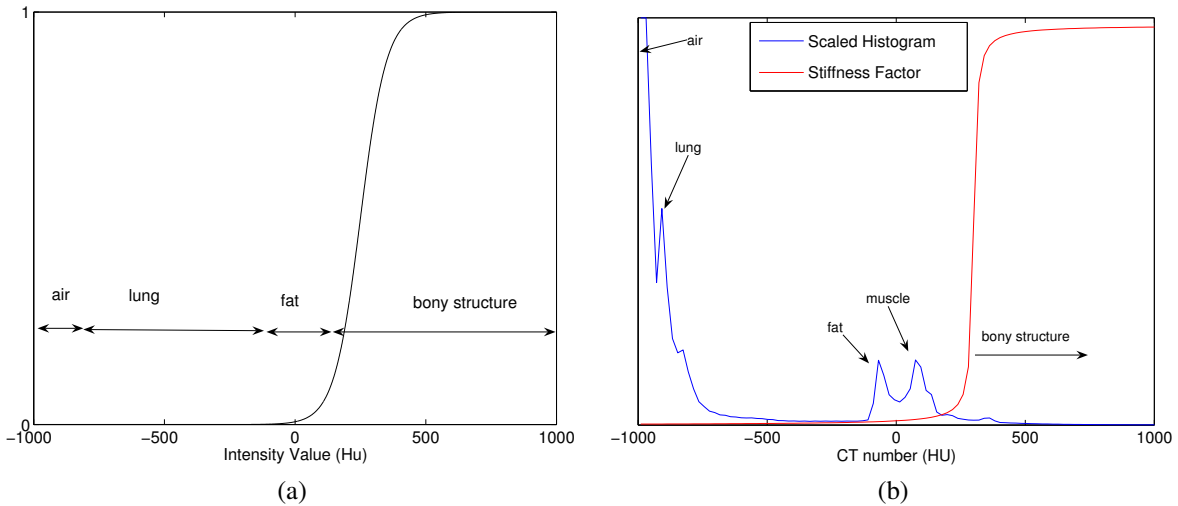


**Figure 1.** Illustration of  $h(\cdot)$ . (a) design of functional  $h$  based on theoretical tissue-type-to-CT-number map; (b) scaled stiffness factor v.s. tissue type information inferred from empirical histogram.

### 2.2.3. Optimization

We adopt the commonly used B-spline basis to parameterize the deformation field  $D$  [9] and solve the optimization problem with the multi-resolution scheme. In particular, we choose

$$D^l(\underline{x}) = \sum_{\underline{i} \in \mathcal{N}(\underline{x})} \theta_{\underline{i}}^l \beta(\underline{x} - \underline{i}).$$

For  $d = 3$  case,  $l \in \{x, y, z\}$  denotes the deformation direction, and separable B-spline basis is used:

$$\beta(\underline{x} - \underline{i}) = \beta\left(\frac{x}{\Delta_x} - i\right)\beta\left(\frac{y}{\Delta_y} - j\right)\beta\left(\frac{z}{\Delta_z} - k\right),$$

where  $\underline{i} = [i, j, k]^T$  denotes the B-spline knot location,  $\Delta_x, \Delta_y, \Delta_z$  determines the scale of B-spline in each direction,  $\underline{x} = [x, y, z]^T$ , and  $\mathcal{N}(\cdot)$  is determined by the support of the B-spline basis.

In each resolution level, we use conjugate gradient method to iteratively solve for the B-spline coefficients until convergence.

## 3. EXPERIMENT SETUP

We tested our approach with two thorax CT scans of the same patient: one at 80% of the vital capacity inhale breath hold (deep inhale breath hold, tidal breathing generally peaks at 40% also) and one at exhale. The scans are both of size  $512 \times 512 \times 148$  with voxel size  $0.2 \times 0.2 \times 0.5 \text{cm}^3$ . We use the deep inhale breath-hold thorax CT image as the reference and further crop it to size  $259 \times 175 \times 107$  to reflect the region of interest. Fig. 2 shows typical data slices (different views) of the reference image, homologous image and the inferred stiffness map ( $h \circ f$ ).

## 4. TEST RESULTS

We first show the registration results in slice views for pure affine transformation and the regularized nonrigid registration method. Deformed homologous image is overlay on top of the reference image for comparison purposes in Fig. 3.

We can observe in Fig. 3 that nonrigid registration has an obvious advantage over global rigid/affine model based registration as far as intensity matching is concerned. Moreover, the better matching result in regions where organs have undergone extremely elastic deformations (like in the diaphragm region). The different performance in the lung area is not obvious due to the fact that the overall intensity level in lung region is pretty low, so mismatch in that region is not emphasized as much as that in high intensity region as far as least squared based similarity metric is concerned. Furthermore, the introduction of proposed tissue type dependent regularization does not seriously deteriorate intensity matching performance in general.

More interestingly, notice that CT number is a very good indicator of tissue type, and bone structures corresponds to high count, we can extract the bony structure by thresholding the CT number to check if our regularization approach has indeed yielded physiologically reasonable results. We extract the geometry from the reference image volume and that of the deformed homologous image, overlay them on top of each other to compare the performance in bone structure alignment. We can clearly observe a nonphysical warping of bones in the deformed homologous geometry using B-spline based nonrigid registration method without the proposed regularization, while affine based registration does not have such an undesirable distortion. This is due to the fact that in the under-determined b-spline nonrigid registration framework, there are many local minima that would yield similar matching result. By taking a close look at where this particular “*bone warping*” phenomena occur, we can see that due to the “*pseudo-periodic*” structure of the ribs, the resulted match and the desired physical one would yield very similar intensity match (data fidelity metric). On the other hand, since B-spline is a local smooth basis, and together with smoothness regularization to enforce continuity of the deformation field, the deformation close to diaphragm/lung region where deformation of more elastic nature occurs, the deformation within bone regions are compromised to resemble those of elastic tissues.

However, when the proposed regularization is applied, the deformation on the bone structures are given an additional “*force*” to conform to rigid transformation. We observe in Fig. 5 an obvious improvement as far as bone-warping issue is concerned.

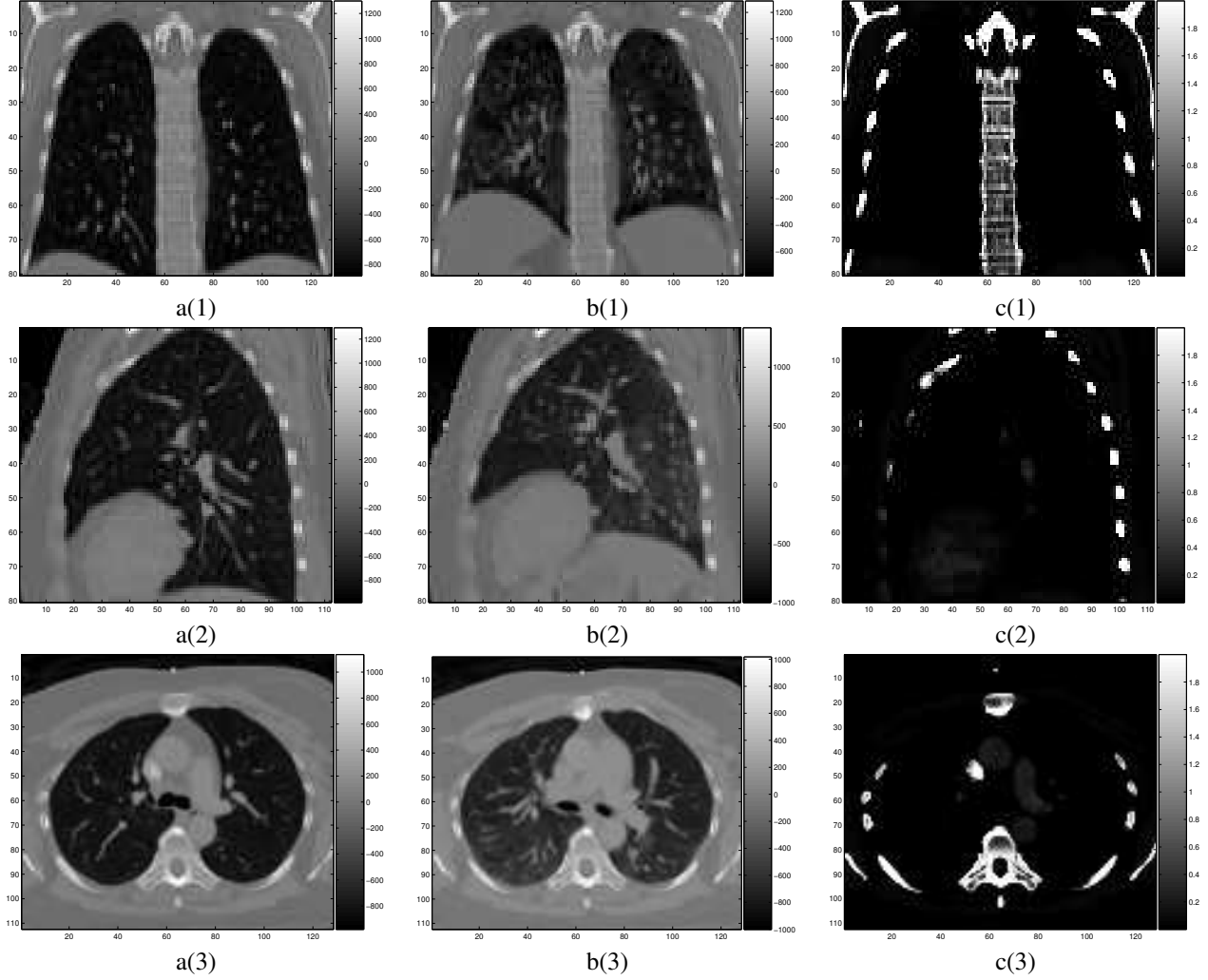


**Figure 2.** Different views of the original data and tissue information inferred from it. Top row [X(1)]: coronal slices; middle row [X(2)]: sagittal slices; bottom row [X(3)]: axial slices. Left column [a(#)]: slices from reference image; middle column [b(#)]: slices from homologous image; right column [c(#)]: slices from inferred stiffness map.

## 5. SUMMARY AND FUTURE WORK

We have proposed a new method to account for tissue-type dependent rigidity information by regularization design in nonrigid registration problem. Experiment with clinical data justifies that the proposed regularization design yields more physiologically sound deformation. As an additive penalty, it acts as a “soft” correcting force in high intensity regions, which tend to correspond to rigid structures towards locally rigid transformations, and relaxes within low intensity regions that tends to correspond to more elastic tissue types.

By designing the local stiffness factor as an implicit function via composition with intensity map, our approach avoids explicit segmentation and is especially robust to partial volume effect, which is important when a multi-resolution technique is to be applied.

Moreover, the design of local rigidity penalty is based on Frobenius norm, and each term involved in evaluating this function and its derivative (which is used in optimization step) is easily available from previous computation of the data fidelity metric. Therefore, the proposed approach hardly incurs any extra computation requirement.

In the future, we will investigate possible quantitative methods to evaluate registration performance besides visual

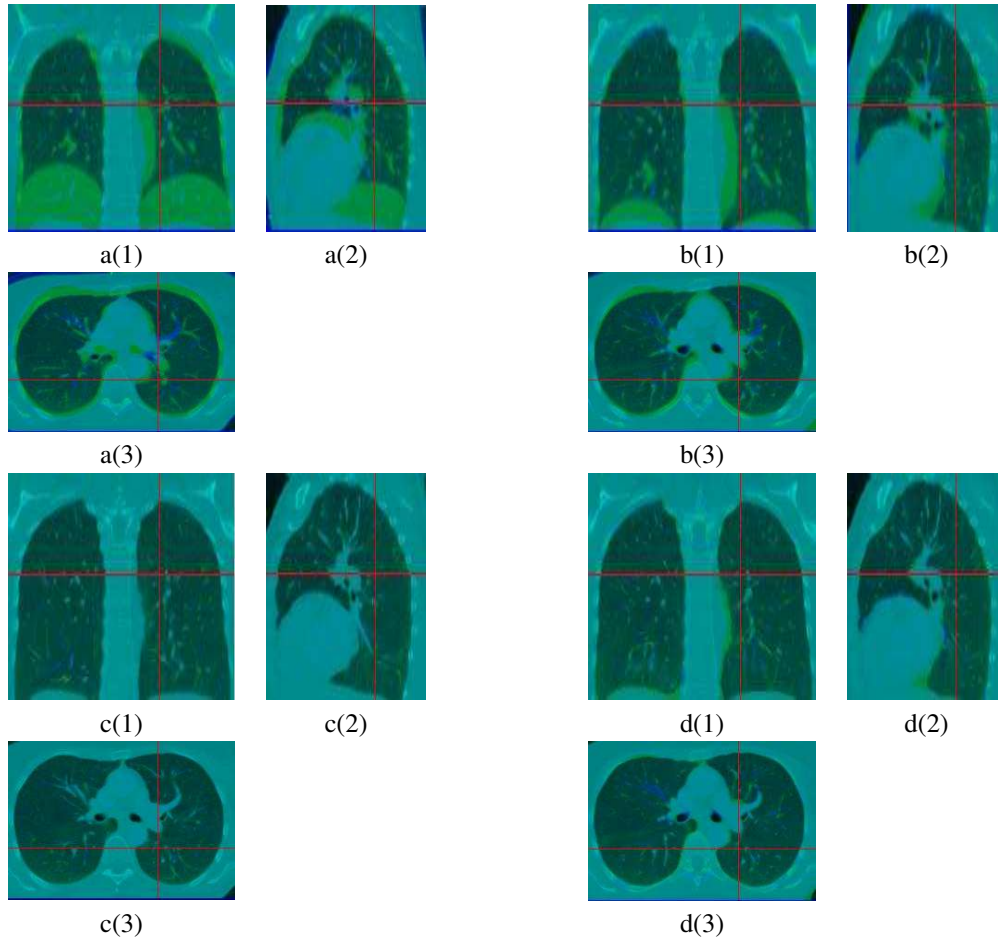


**Figure 3.** Deformed homologous image (green) overlaid with reference image (dark blue) for comparison of intensity match. Different views are indicated with numbers: [X(1)] coronal view; [X(2)] sagittal view; [X(3)] axial view [X(3)]. Different registration method are distinguished with letters: [a(#)] rigid transformation model; [b(#)] affine transformation model; [c(#)] B-Spline registration with smoothness penalty only; [d(#)] B-Spline registration with both proposed regularization.

justification that would provide better physiological interpretation of the alignment results. We will further study the trade-off between data fidelity metric and prior knowledge guided term (penalty/regularization). Finally, we would like to generalize this method to other modalities where there is no explicit relationship between observation and tissue type dependent stiffness factors.

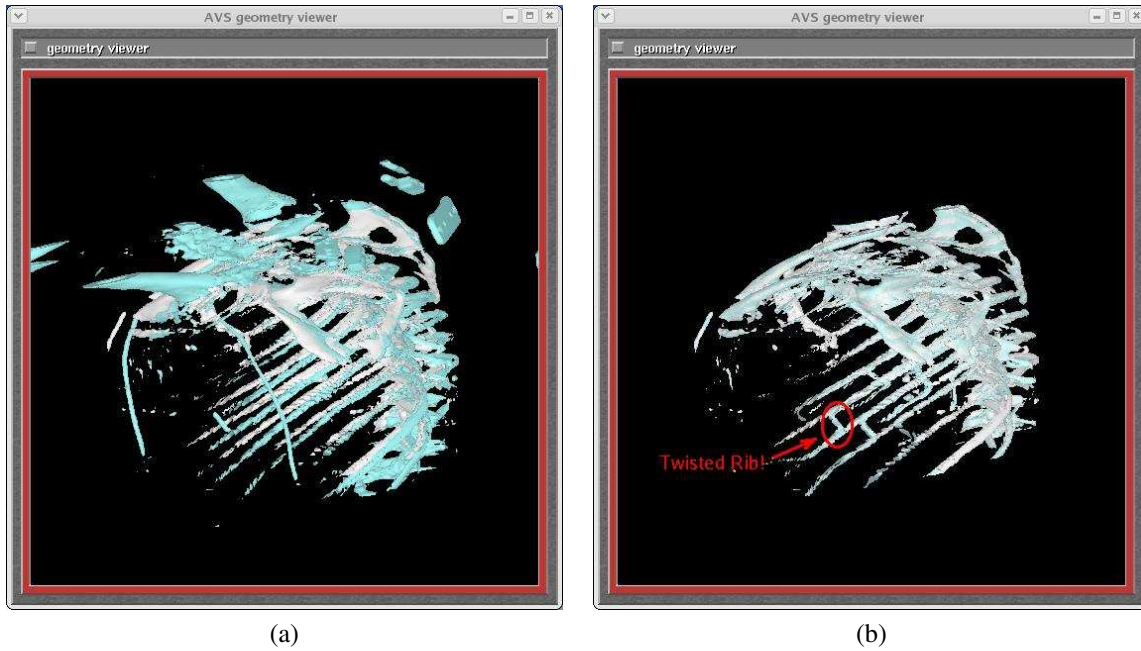


**Figure 4.** Geometry extracted (a) unregistered images; (b) B-Spline based registration with homogeneous smoothness regularization only.

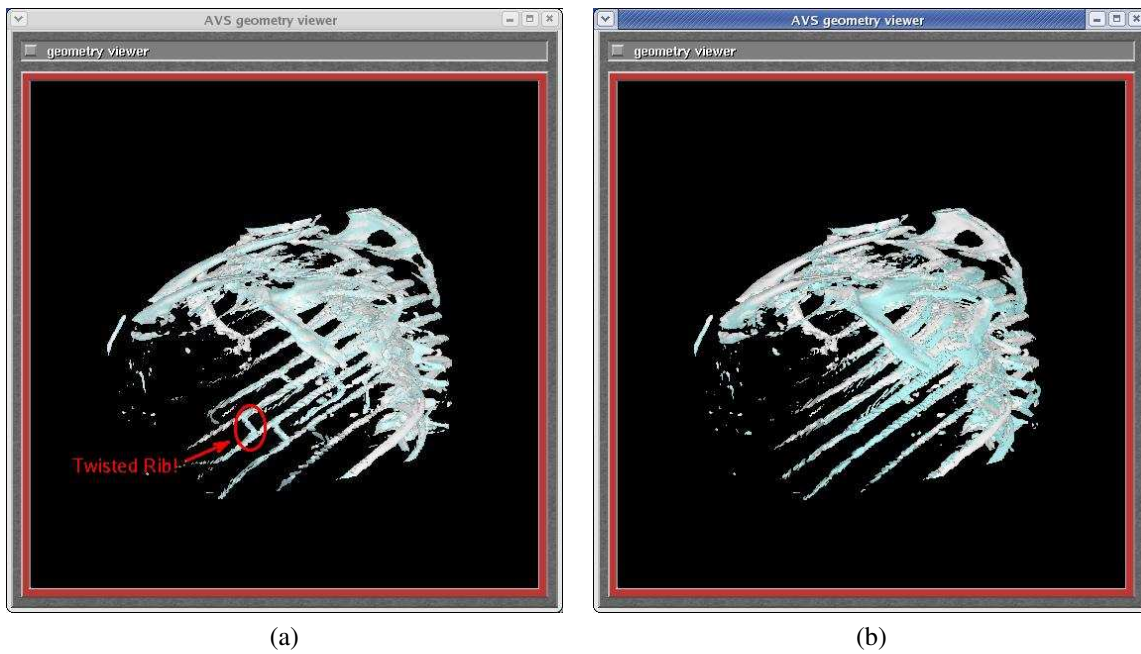


**Figure 5.** Geometry extracted from registration results: (a) B-Spline based nonrigid registration with no local rigidity regularization; (b) B-Spline based nonrigid registration result with proposed local tissue type dependent regularization.

### ACKNOWLEDGMENTS

This work is supported in part by NIH grant P01-CA59827.



## REFERENCES

1. J. B. A. Maintz and M. A. Viergever, "A survey of medical image registration," *Med. Im. Anal.* **2**, pp. 1–36, Mar. 1998.
2. T. Rohlfing, C. R. Maurer, D. A. Bluemke, and M. A. Jacobs, "Volume-preserving nonrigid registration of MR breast images using free-form deformation with an incompressibility constraint," *IEEE Tr. Med. Im.* **22**, pp. 730–741, June 2003.
3. B. Karacali and C. Davatzikos, "Topology preservation and regularity in estimated deformation fields," in *Information Processing in Medical Im.*, pp. 426–37, 2003.
4. B. Karacali and C. Davatzikos, "Estimating topology preserving and smooth displacement fields," *IEEE Trans. Med. Imag.* **23**, pp. 868–80, July 2004.
5. J. A. Little, D. L. G. Hill, and D. J. Hawkes, "Deformations incorporating rigid structures," *IEEE Tr. Nuc. Sci.* **66**, pp. 223–232, May 1997.
6. R. H. Huesman, G. J. Klein, J. A. Kimdon, C. Kuo, and S. Majumdar, "Deformable registration of multimodal data including rigid structures," *IEEE Tr. Nuc. Sci.* **50**, pp. 389–92, June 2003.
7. M. Staring, S. Klein, and J. P. Pluim, "Nonrigid registration with adaptive, content-based filtering of the deformation field," in *Proc. SPIE 5747, Medical Imaging 2005: Image Proc.*, pp. 212–21, 2005.
8. J. Hsieh, *Computed tomography: Principles, design, artifacts, and recent advances*, SPIE, Bellingham, 2003.
9. J. Kybic and M. Unser, "Fast parametric elastic image registration," *IEEE Tr. Im. Proc.* **12**, pp. 1427–42, Nov. 2003.